Appl Phys B (2009) 94: 437–441
DOI 10.1007/s00340-008-3351-5

Applied Physics B
Lasers and Optics

Growth and magneto-optical properties of $LiTb(MoO_4)_2$ crystal

F. Guo · J. Ru · H. Li · N. Zhuang · B. Zhao · J. Chen

Received: 18 June 2008 / Revised version: 5 November 2008 / Published online: 20 December 2008

Abstract Lithium terbium molybdate ($LiTb(MoO_4)_2$) single crystal was grown by the Czochralski method. The lattice parameters of the crystal were determined by X-ray diffraction analysis. The absorption coefficient and the Faraday rotation spectrum ($B = 1.07$ T) were investigated at wavelengths of 400–1500 nm at room temperature. Verdet constants of $LiTb(MoO_4)_2$ crystal at 532-, 633- and 1064-nm wavelengths were measured by the extinction method. The results show that $LiTb(MoO_4)_2$ crystal has a larger magneto-optical figure of merit than that of terbium gallium garnet at wavelengths of 600–1500 nm.

PACS 78.20.Ls · 81.10.Fq

1 Introduction

Inorganic solids with large Faraday effects can be practically utilized as optical isolators, optical modulators, sensors of electrical current, sensors of magnetic field and so forth [1]. Faraday isolators are a key component of many contemporary laser systems. Due to recent progress in laser applications such as precise measurements and advanced display systems, the demand for optical Faraday devices is increasing at wavelengths of 400–1100 nm, where conventional yttrium iron garnets (YIG) and doped YIG are not applicable because of their poor transparency. For these devices, both large Faraday rotation (FR) angles and high transmittance are important. Terbium gallium garnet (TGG) is thought to be the better material for such requirements among transparent magnetic materials because of its large Verdet constant [2, 3] and good transmittance [4]. TGG crystal can be grown by the Czochralski technique [4]; however, the relatively high decomposition and evaporation of Ga_2O_3 from the melt cause some difficulties during TGG crystal growth [5].

The Tb^{3+} ion exhibits a strong paramagnetism due to the transition $4f^8$–$4f^7 5d$ [6]. $NaTb(WO_4)_2$ crystal was reported to have larger Verdet constant and magneto-optical figure of merit than those of TGG in the visible and near-infrared regions [7]. In the last few years, molybdate crystals with general formula $MRE(MoO_4)_2$ (M = alkali metal, RE = rare earth) are attractive host materials for their large lanthanide admittance [8–13]. In this work, we study the growth and magneto-optical properties of $LiTb(MoO_4)_2$ crystal.

2 Experimental

2.1 Crystal growth

The polycrystalline materials for crystal growth were prepared by solid-state reaction according to the following chemical reaction equation:

$$2Li_2CO_3 + Tb_4O_7 + 8MoO_3 \rightarrow 4LiTb(MoO_4)_2 + CO_2\uparrow + 1/2O_2\uparrow. \quad (1)$$

Stoichiometric amounts of Tb_4O_7 (5N), Li_2CO_3 (3N) and MoO_3 (3N) were weighed accurately with addition of 1.5 wt% excess MoO_3 to compensate for its volatilization loss during the process of crystal growth. These chemicals were mixed and pressed into tablets, and then the tablets were sintered at 850°C for 20 h in air.

F. Guo · J. Ru · H. Li · N. Zhuang · B. Zhao · J. Chen (✉)
College of Chemistry and Chemical Engineering, Fuzhou University, Fuzhou 350002, China
e-mail: j.z.chen@fzu.edu.cn
Fax: +86-591-22866232

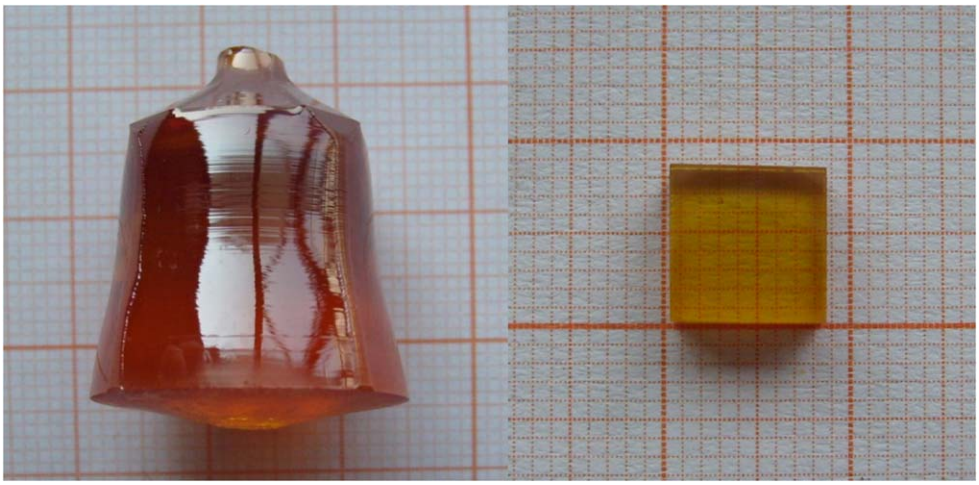

Fig. 1 As-grown crystal of $LiTb(MoO_4)_2$

The $LiTb(MoO_4)_2$ crystal was grown by the Czochralski method, in a Φ 55 mm × 35 mm platinum crucible with radio frequency (RF) induction heating. It was grown in the ⟨001⟩ direction at a pulling rate of 1.0 mm/h and a rotating rate of 10–15 rpm. Finally, $LiTb(MoO_4)_2$ crystal with dimensions of Φ 18 mm × 30 mm was obtained, as shown in Fig. 1, which is yellowish-brown and crack free.

2.2 X-ray powder diffraction

The X-ray powder diffraction measurement was carried out by a computer-automated diffractometer (Rigaku D/max-3c) equipped with Cu Kα radiation ($\lambda = 1.54056$ Å) at room temperature. The measured diffraction data of $LiTb(MoO_4)_2$ were refined through an external standard method and an internal standard method with standard Si powder.

2.3 Transmission spectrum

The grown $LiTb(MoO_4)_2$ single crystal was cut along the ⟨001⟩ plane, which was oriented by X-ray diffraction (XRD), and then ground and polished carefully to about 4-mm thickness for spectral measurement. The transmission spectrum was measured using a Perkin–Elmer Lambda 900 spectrophotometer over the wavelength range 400–1500 nm at room temperature. The transmission spectrum of TGG was also measured for comparison (a commercial device-quality TGG sample was supplied by Fuzhou TCT Co.).

2.4 FR measurement

FR of $LiTb(MoO_4)_2$ crystal in the direction of the optical axis was measured at room temperature by the extinction method [7]. In this measurement, lasers of 532-, 633- and 1064-nm wavelengths were used as the sources of probe light. Magnetic intensity was adjusted from 0 to 1.2 T continuously.

In order to indicate the relationship between FR and wavelength, FR spectra at a constant field ($B = 1.07$ T) were measured over the wavelength range 400–1500 nm at room temperature. Two polarizers and NdFeB permanent magnets were placed on the testing platform of the Perkin-Elmer Lambda 900 UV-VIS-NIR spectrophotometer. The polarizing directions of the two polarizers are parallel. Transmission spectra of $LiTb(MoO_4)_2$ and TGG crystals with and without NdFeB permanent magnets were measured over the wavelength range 400–1500 nm at room temperature.

3 Results and discussion

3.1 Lattice parameters

The unit-cell parameters were determined with the help of a computer program. The result shows that the crystal $LiTb(MoO_4)_2$ belongs to the tetragonal system and the unit-cell parameters are $a = b = 0.5179(2)$ nm, $c = 1.1300(5)$ nm and $V = 0.3031(4)$ nm^3. The patterns of X-ray powder diffraction were indexed, as shown in Fig. 2.

3.2 Absorption coefficient

Figure 3 shows the transmission spectra of $NaLi(MoO_4)_2$ and TGG crystals. The absorption peak around 488 nm corresponds to the Tb^{3+} ion $^7F_6 \rightarrow {}^5D_4$ transition line in the crystal; the sharp absorption region is usually avoided in practice.

The absorption coefficient α was calculated by McLean's formula [14]:

$$T = \frac{(1 - R^2)\exp(-\alpha d)}{1 + R^2\exp(-2\alpha d)}, \tag{2}$$

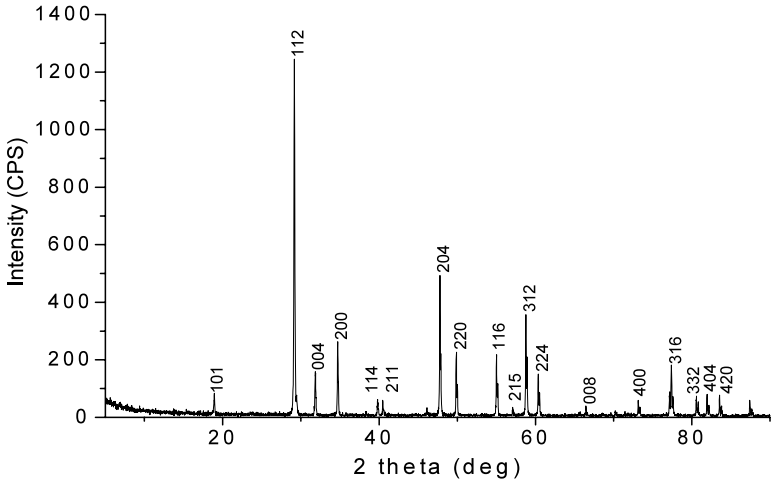

Fig. 2 XRD patterns of $LiTb(MoO_4)_2$ crystal at room temperature

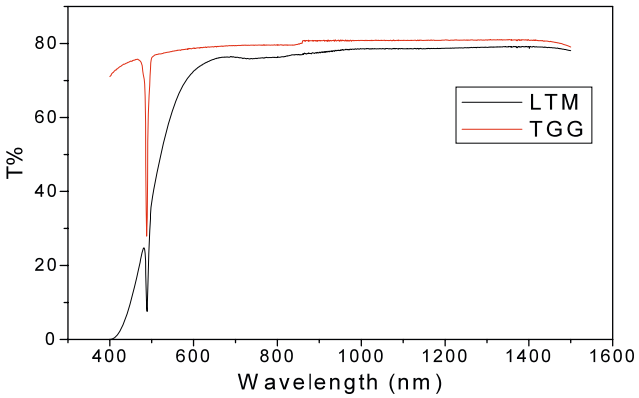

Fig. 3 Transmission spectra of $LiTb(MoO_4)_2$ and TGG crystals at room temperature

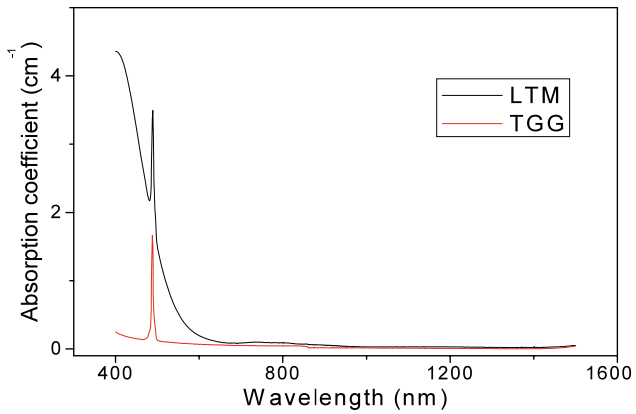

Fig. 4 Absorption spectra of $LiTb(MoO_4)_2$ and TGG crystals

where T is the transmission coefficient, d is the specimen thickness and R is the dispersion of the reflection coefficient, which can be calculated from the reflective index. Absorption loss is an important parameter of magneto-optical properties. Figure 4 indicates that $LiTb(MoO_4)_2$ has a small absorption loss in the 600–1500 nm wavelength range.

3.3 Verdet constant

As is well known, FR in a material is given by the equation

$$\theta = VHL, \tag{3}$$

where θ is the rotation angle, L is the length of the light path in a medium, H is the magnetic field applied along the light beam and V is the Verdet constant. FR angles at a specified wavelength are proportional to the magnetic intensity. The straight lines were fitted using a computer program, as demonstrated in Fig. 5. The Verdet constants can be calculated by the slope of straight lines. They are listed in Table 1. At the same time, the Verdet constants of TGG are also given in Table 1, which came from Refs. [3, 15].

3.4 FR spectrum

The FR spectrum can be calculated by the following formula:

$$\theta_\lambda = \frac{180 \times \arccos(I/I_0)}{\pi \times L}, \tag{4}$$

where I_0 is the intensity of transmitted light without applying a magnetic field and I is the intensity of transmitted light with applying a magnetic field. The calculated Faraday rotation spectra of $LiTb(MoO_4)_2$ and TGG are shown in Fig. 6. Compared to the FR of TGG, $LiTb(MoO_4)_2$ has a larger FR at wavelengths of 400–1500 nm (absolute value).

Magneto-optical properties of RE compounds are closely connected with their magnetic properties [16]. Van Vleck and Hebb [17] derived the following relationship between the paramagnetic Verdet constant and the magnetic susceptibility χ for a free ion:

$$V = \chi K_0 g^{-1}\left[1 - \frac{\lambda^2}{\lambda_0^2}\right]^{-1}, \tag{5}$$

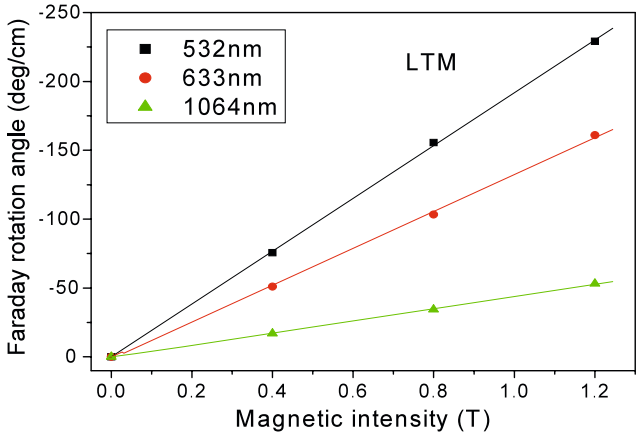

Fig. 5 Relationship between FR and magnetic intensity of $LiTb(MoO_4)_2$ crystal

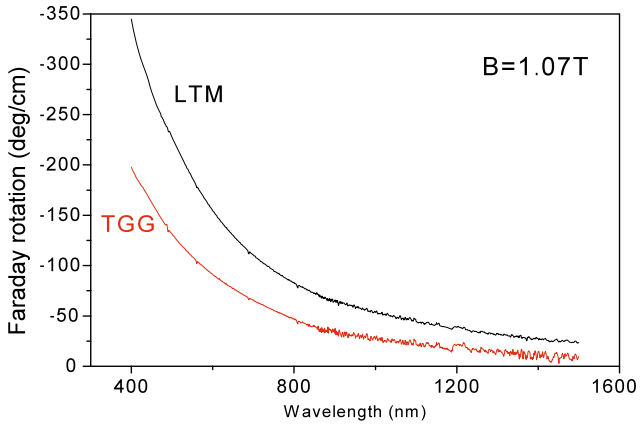

Fig. 6 FR spectra of $LiTb(MoO_4)_2$ and TGG crystals

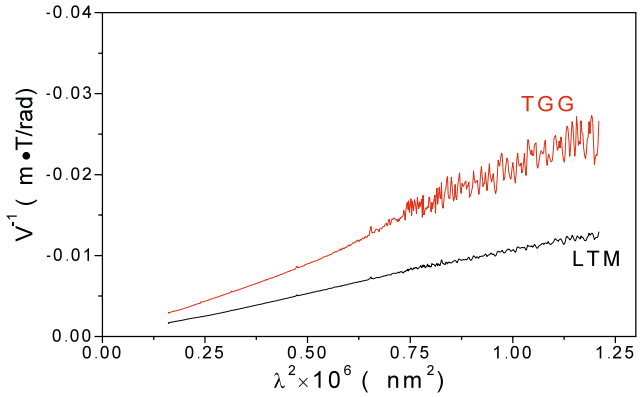

Fig. 7 Relationship between V^{-1} and λ^2 of $LiTb(MoO_4)_2$ and TGG crystals

where g is the Lande factor of the ground-state splitting, λ_0 is the wavelength of the effective electron transition equivalent in action to all transitions, producing FR far enough from the resonance absorption, and K_0 is a coefficient of

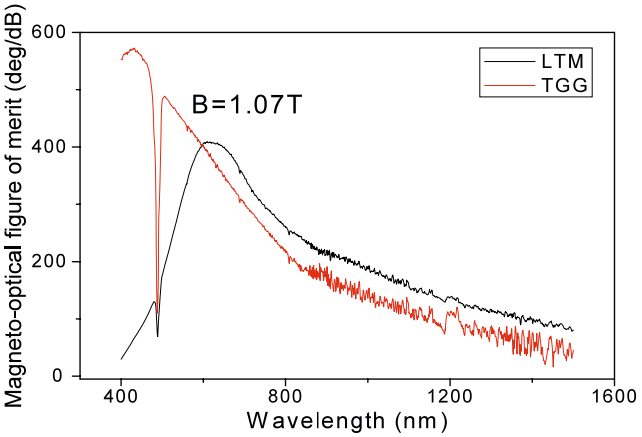

Fig. 8 Spectra of magneto-optical figure of merit for $LiTb(MoO_4)_2$ and TGG crystals

Table 1 Verdet constants of $LiTb(MoO_4)_2$ and TGG crystals

Crystal	$LiTb(MoO_4)_2$			TGG		
Wavelength (nm)	532	633	1064	532	633	1064
Verdet constants (rad/mT)	−335	−233	−76	−190		−134
				−40		

proportionality between the magneto-optical activity of the effective transition and the magnetic susceptibility.

The reciprocal of V in (5) is written as

$$V^{-1} = g\left(1 - \frac{\lambda^2}{\lambda_0^2}\right)/\chi K_0 \equiv B_0\left(\lambda^2 - \lambda_0^2\right), \tag{6}$$

where B_0 is a negative constant. Figure 7 shows the relationship between V^{-1} and λ^2 for $LiTb(MoO_4)_2$ and TGG crystals. Although there is some non-linearity for the two crystals in the graph of V^{-1} vs λ^2, this is different from that of Tb^{3+} ions embedded in glass systems [18]. It shows that the CF contribution to the Verdet constant of magneto-optical crystals should not be ignored [19].

3.5 Magneto-optical figure of merit

The magneto-optical figure of merit, defined by the ratio of FR and optical absorption loss, can generally represent the magneto-optical properties of materials [20]. The result shows that $LiTb(MoO_4)_2$ has a larger magneto-optical figure of merit than that of TGG at wavelengths of 600–1500 nm. Because the absorption coefficient increases, the magneto-optical figure of merit of $LiTb(MoO_4)_2$ decreases at wavelengths of 400–600 nm obviously, as shown in Fig. 8.

4 Conclusions

$LiTb(MoO_4)_2$ crystal has been grown successfully by the Czochralski method. The crystal has a larger specific FR than that of TGG at wavelengths of 400–1500 nm and a larger magneto-optical figure of merit than that of TGG at wavelengths of 600–1500 nm. So, $LiTb(MO_4)_2$ can be a good candidate material for magneto-optical devices in the visible and near-infrared regions.

Acknowledgements This work is supported by the National Natural Science Foundation of China (50772023), the Natural Science Foundation of Fujian Province (2007J0148) and the Open Fund of the National Photonic Crystal Materials Engineering and Technology Research Center (07h3561xaa), respectively.

References

1. K. Tanaka, N. Tatehata, K. Fujita, K. Hirao, N. Soga, J. Phys. D: Appl. Phys. **31**, 2622 (1998)
2. C.B. Rubinstein, L.G. Van Uitert, W.H. Grodkiewicz, J. Appl. Phys. **35**, 3096 (1964)
3. M.Y.A. Raja, D. Allien, W. Sisk, Appl. Phys. Lett. **67**, 2123 (1995)
4. B. Sugg, H. Nürge, B. Faust, E. Ruza, R. Niehüser, H.-J. Reyher, R.A. Rupp, L. Aclerman, Opt. Mater. **4**, 354 (1995)
5. C.R. Linares, Solid State Commun. **2**, 229 (1964)
6. N. Sawanobori, N. Mori, D. Imaizumi, New Glass **18**, 5 (2003)
7. J. Liu, F. Guo, B. Zhao, N. Zhuang, Y. Chen, Z. Gao, J. Chen, J. Cryst. Growth **310**, 2613 (2008)
8. A.A. Kaminskii, *Laser Crystals. Their Physics and Properties*, 2nd edn. Springer Ser. Opt. Sci., vol. 14 (Springer, Berlin, 1990)
9. S.B. Stevens, C.A. Morrison, T.H. Allik, A.L. Rheingold, B.S. Haggerty, Phys. Rev. B **43**, 7386 (1991)
10. Yu.K. Voron'ko, K.A. Subbotin, V.E. Shukshin, D.A. Lis, S.N. Ushakov, A.V. Popov, E.V. Zharikov, Opt. Mater. **29**, 246 (2006)
11. X.Z. Li, Z.B. Lin, L.Z. Zhang, G.F. Wang, J. Cryst. Growth **293**, 157 (2006)
12. X.A. Lu, Z.Y. You, J.F. Li, Z.J. Zhu, G.H. Jia, B.C. Wu, C.Y. Tu, J. Alloys Compd. **426**, 352 (2006)
13. V. Volkov, C. Cascales, A. Kling, C. Zaldo, Chem. Mater. **17**, 291 (2005)
14. V. Marinova, M. Veleva, Opt. Mater. **19**, 332 (2002)
15. D.I. Dentz, R.C. Puttbach, R.R. Belt, Proc. AIP Conf. **18**, 954 (1974)
16. A. Potseluyko, I. Edelman, A. Malakhovskii, Y. Yeshurun, T. Zarubina, A. Zamkov, A. Zaitsev, Microelectron. Eng. **69**, 216 (2003)
17. J.H. Van Vleck, M.H. Hebb, Phys. Rev. **46**, 17 (1934)
18. J. Qiu, K. Tanaka, N. Sugimoto, K. Hirao, J. Non-Cryst. Solids **213–214**, 193 (1997)
19. A.V. Malakhovskii, Phys. Status Solidi B **159**, 883 (1990)
20. M. Huang, Z.-C. Xu, Thin Solid Films **450**, 324 (2004)